IEEE Access
Multidisciplinary | Rapid Review | Open Access Journal

Received March 10, 2021, accepted April 4, 2021, date of publication April 12, 2021, date of current version April 19, 2021.

Digital Object Identifier 10.1109/ACCESS.2021.3072783

Exploring the Limits of a Redundant Actuation System Through Co-Design

GIANLUIGI GRANDESSO[1], GABRIEL BRAVO-PALACIOS[2], (Graduate Student Member, IEEE), PATRICK M. WENSING[2], (Member, IEEE), MARCO FONTANA[3], (Member, IEEE), AND ANDREA DEL PRETE[1], (Member, IEEE)

[1]Department of Industrial Engineering, University of Trento, 38123 Trento, Italy
[2]Department of Aerospace and Mechanical Engineering, University of Notre Dame, Notre Dame, IN 46556, USA
[3]TeCIP Institute, Scuola Superiore Sant'Anna, 56127 Pisa, Italy

Corresponding author: Gianluigi Grandesso (gianluigi.grandesso@unitn.it)

This work was supported by the Italian Ministry for Education, University, and Research (MIUR) through the Departments of Excellence Program.

ABSTRACT This paper assesses the energy efficiency of a redundant actuation architecture combining Quasi-Direct Drive (QDD) motors and Series Elastic Actuators (SEAs) by comparing its energy consumption to Geared Motors (GMs) and SEAs alone. We consider this comparison for two robotic systems performing different tasks. Our results show that using the redundant actuation we can save up to 99% of energy with respect to SEA for sinusoidal movements. This efficiency is achieved by exploiting the coupled dynamics of the two actuators, resulting in a latching-like control strategy. We also show that these large energy savings are not straightforwardly extendable to nonsinusoidal movements, but smaller savings (*e.g.*, 7%) are nonetheless possible. The presented results were obtained thanks to the framework of concurrent design (co-design), namely the simultaneous optimization of hardware parameters and control trajectories. This shows that the combination of complex hardware morphologies and advanced numerical co-design can lead to peak hardware performance that would be unattainable by human intuition alone.

INDEX TERMS Co-design, optimization, redundant actuator, series elastic actuator (SEA), quasi-direct drive (QDD).

I. INTRODUCTION

In the last decades, many roboticists focused their research on determining which actuation mechanisms are most suitable for robotic systems such as legged robots or industrial manipulators [1]–[5]. Often, the ''stiffer is better'' rule of thumb has been adopted as a premise of the design process. High bandwidth force control and accurate position control are the two main benefits, however to the detriment of safety in human-machine interactions and high cost of the mechanical system. While active control is able to regulate output impedance, there are fundamental limits to mechanical robustness in the case of impulsive loads. Thus, many have taken inspiration from nature, intentionally including compliance in actuation systems between the load and mechanical energy source.

The associate editor coordinating the review of this manuscript and approving it for publication was Okyay Kaynak.

To date, there is no actuation mechanism that uniformly outperforms the others. This is due to the strong dependency on the task (*e.g.*, walking, holding objects, pick-and-place operations) that the system has to perform, and on the environment (*e.g.*, structured, unknown, with humans) in which it operates. Moreover, relative performance depends heavily on the performance index (*e.g.*, energy consumption, task completion time, accuracy) that is considered. Thus, in the robot design process, many factors have to be weighed and designers inevitably have to deal with many trade-offs.

Among those actuation mechanisms that use DC motors, the two that are most often employed are Series Elastic Actuation (SEA) [6] and Quasi-Direct Drive (QDD) motors [7] (*i.e.*, low-gear-ratio actuators). In an SEA, the motor is connected to a gearbox, which in turn is attached to one end of a spring, with the other end of the spring attached to the joint output. In terms of benefits, SEAs provide mechanically passive energy storage and regeneration, impact mitigation, high

output torque, and increased peak output power. Moreover, an SEA can provide low mechanical output impedance, good force controllability, and safety in human-machine interactions. On the other hand, the drawbacks of SEAs include low control bandwidth and difficulty in controlling impulsive movements [1], [2], [6], [8].

A QDD motor instead is simply a Geared Motor (GM) with reduced gear ratio, limited to roughly 10:1. In QDD actuation, the low-reduction transmission results in good transparency: low backlash, back-driveability, reduced reflected inertia of the motor, and lower friction (*i.e.*, higher power transmission efficiency). Moreover, QDD actuators have high control bandwidth, active compliance tuning capabilities, and good position controllability. Of course there are disadvantages in using QDD motors, such as low output torque and high Joule heating due to the necessity of working in high-current regimes [7]–[9].

Considering advantages and disadvantages of the two actuation mechanisms, there is a certain degree of complementarity between QDD and SEA. Recently, some researchers investigated the idea of exploiting the benefits of these two design approaches developing a high-bandwidth redundant actuator [8], [9] that uses QDD motors and SEA in parallel, as illustrated in Fig. 1. The results are promising, but it is still unclear whether this redundant actuation is energetically more efficient than SEA or QDD/GM alone.

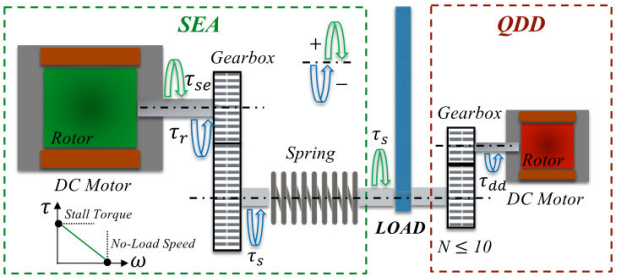

FIGURE 1. Schematic of the redundant actuation system: an SEA and a QDD work in parallel to actuate a single revolute joint.

In order to fairly consider the performance limitations of these systems, we propose a framework to optimize design parameters using co-design, which simultaneously considers hardware and control in the design process. This means that hardware parameters (*e.g.*, spring stiffness, gear ratio) are included in an optimal control problem (OCP) as variables to be optimized, such that the final output is an actuation system that minimizes the energy consumed to perform a specific task. This approach, introduced for the first time in 1994 in computer graphics by Sims [10], overcomes the problems affecting the classic iterative robot design process, which relies heavily on expert knowledge, and can be highly inefficient in terms of time, cost, and final performance.

A key required aspect of the co-design framework is the definition of objectives. In a robot design process, defining goals in terms of objective functions allows for an assessment of the robot performance. This makes co-design a rigorous approach for parametric design optimization, enabling designers to obtain optimized designs tailored to specific tasks. A number of publications have shown the potential of co-design [11]–[16], which proves its maturity for our case study.

The contribution of this paper is a systematic design study for this redundant actuation architecture—demonstrating how, where, and when it will provide energetic benefits over SEA or GM alone. In further detail, we list here our main findings.

1) For sinusoidal motions, our analysis shows that a latching-like control strategy (*i.e.*, keeping the SEA rotor velocity in counter-phase with the joint velocity), similar to the one employed in energy harvesters [17], [18], is optimal using the redundant actuation, which is able to save up to 99% of energy compared to SEA.
2) For nonsinusoidal motions, we show that these large energy savings are not straightforwardly extendable. Nonetheless, the redundant actuators can still be more energy efficient than SEA (*e.g.*, 7%), especially for proximal joints, where the weight of the actuator at the base does not contribute to the robot inertia.
3) We have studied the closed-loop behavior of the redundant actuator under perturbations. These results show that in some tasks the actuation redundancy can also help track the desired trajectories while maintaining low energy consumption.

II. METHODS

This research starts from the analysis of the redundant actuation applied to a 1 degree of freedom (DoF) system and then extends the study to a 2-DoF manipulator. The analysis of the 1-DoF system compares the energy consumption of this actuation, considering a DD motor instead of a QDD for simplicity, with that of an SEA. In particular, considering a periodic sinusoidal motion with fixed amplitude, we investigated the variation of consumed energy as function of the oscillation frequency and other hardware parameters.

Then, we carried out the same comparative analyses of energy consumption with the 2-DoF manipulator for two specific tasks: the classic swing-up problem, and a pick-and-place operation. In addition, following a co-design approach, we included some hardware parameters as decision variables of the optimization problem. This illustrates how co-design may be a suitable way to design highly-efficient manipulators, considering both hardware and control.

A. 1-DoF: MODEL

As schematized in Fig. 1, the 1-DoF system with redundant actuation consists of a link connected to the ground by a revolute joint, which is actuated simultaneously by a DD motor and an SEA. The DD acts directly on the joint, while the SEA motor is connected to it by a gearbox and a torsional spring. The link dynamics is:

$$I_l\,\ddot{\theta}(t) = \tau_s(t) - m\,g\,\cos\left(\theta(t)\right)\,\frac{l}{2} + \tau_{dd}(t), \qquad (1)$$

where $\theta(t)$ is the link angle, I_l denotes its rotational inertia around the revolute joint, m is its mass, l its length and g is gravity. $\tau_s(t)$ and $\tau_{dd}(t)$ are respectively the output torque of the SEA spring and the DD motor. The case with only SEA was considered setting $\tau_{dd}(t) = 0$.

The dynamics of the SEA motor instead is:

$$I_{se}\,\ddot{\theta}_{se}(t) = \tau_{se}(t) - \tau_r(t), \tag{2}$$

where $\theta_{se}(t)$ is the SEA motor angle, $\tau_{se}(t)$ is the torque generated by the SEA motor and $\tau_r(t)$ is the load torque acting on the SEA motor. For the 1-DoF case, the spring pre-load was set to zero. The dynamics of the SEA motor is coupled with that of the link by means of the SEA gearbox and spring:

$$\tau_r(t) = \frac{1}{N\eta} K_s \left(\frac{\theta_{se}(t)}{N} - \theta(t) \right), \tag{3}$$

with K_s the SEA spring stiffness, N the gear ratio of the SEA gearbox, and η its efficiency [2], which accounts for the torque-dependent friction losses inside the gearbox. Note that $\tau_s(t) = N\eta\tau_r(t)$. For the sake of simplicity, the dependency of the efficiency on the gearbox loading was neglected, as well as the fact that when the motor is not active ($\tau_{se}(t) = 0$) then the inefficiency would increase the braking capability. Indeed, modelling the gearbox efficiency as a factor multiplying the gear ratio makes the breaking torque zero when the motor is not active, which is not true for a real geared transmission subject to friction. To further simplify the analysis in the 1-DoF case, the inertias associated with the DD motor and with the SEA gearbox were not taken into account, assuming that they are dominated respectively by the inertia of the link (about four orders of magnitude lower) and that of the SEA motor (about one order of magnitude lower). Finally, in this simple 1-DoF case, only the thermal losses of the motors were considered, neglecting Coulomb and viscous friction.

B. 1-DoF: OCP FOR DETERMINING MINIMAL ENERGY CONTROLS

The motion that was chosen for this analysis is a simple sinusoid with fixed amplitude $A = 5°$ and frequency f around the vertical position of the link, *i.e.*, $\theta(t) = \pi/2 + A\sin(ft)$. A small oscillation amplitude was chosen to limit the required motor torque at high frequencies. Enforcing this movement, the system of equations (1)-(3) is determined and can be solved analytically in the case with only the SEA, since the only control variable is the SEA motor torque. Therefore, if a solution exists it is unique.

Considering the redundant actuation instead, the system of equations becomes under-determined because of the DD motor torque. Thus, we formulated an OCP to realize the desired motion of the link with the least amount of energy:

$$\underset{x(\cdot),u(\cdot)}{\text{minimize}} \;\; \Phi\,(x(\cdot), u(\cdot)) \tag{4a}$$
$$\text{subject to } \dot{x}(t) = f(t, x(t), u(t)) \tag{4b}$$
$$h(t, x(t), u(t)) \leq 0 \tag{4c}$$
$$g(t_f, x(0), x(t_f)) \leq 0 \tag{4d}$$

The state and control trajectories, with values $x(t) \in \mathbb{R}^n$ and $u(t) \in \mathbb{R}^m$, are the decision variables. The objective function is represented by $\Phi(\cdot)$, while the dynamics, path and boundary constraints respectively by (4b), (4c) and (4d).

For the cost function, we chose the energy consumed to complete a cycle such that the time horizon is $t_f = 2\pi/f$. We initially neglected any capability to regenerate energy from braking:

$$\Phi\,(\cdot) = \int_0^{t_f} \max(0, P_{se}(t)) + \max(0, P_{dd}(t))\; dt, \tag{5}$$

with P_{se} and P_{dd} the power associated respectively to the SEA and the DD motor, expressed as:

$$P_{se}(t) = \tau_{se}(t)\,\dot{\theta}_{se}(t) + \frac{\tau_{se}(t)^2}{K_m} \tag{6}$$
$$P_{dd}(t) = \tau_{dd}(t)\,\dot{\theta}(t) + \frac{\tau_{dd}(t)^2}{K_m}, \tag{7}$$

and where K_m denotes the motor constant. The introduction of the $\max(\cdot)$ function would cause numerical problems because of its non-differentiability at zero. To avoid this non-smooth cost, we reformulated the cost by introducing two additional variables, $\epsilon_{se}(t)$ and $\epsilon_{dd}(t)$:

$$\Phi(\cdot) = \int_0^{t_f} \frac{P_{se}(t) + \epsilon_{se}(t)}{2} + \frac{P_{dd}(t) + \epsilon_{dd}(t)}{2}\; dt \tag{8}$$

while enforcing the constraints

$$\epsilon_{se}(t) \geq -P_{se}(t), \quad \epsilon_{se}(t) \geq P_{se}(t) \tag{9}$$
$$\epsilon_{dd}(t) \geq -P_{dd}(t), \quad \epsilon_{dd}(t) \geq P_{dd}(t) \tag{10}$$

With this formulation, when $P < 0$ the solver optimizes to $\epsilon = -P$ so that $\frac{P+\epsilon}{2} = 0$. When instead $P \geq 0$ the solver optimizes to $\epsilon = P$ so that $\frac{P+\epsilon}{2} = P$.

We also considered the case of energy regeneration, accounting for a battery that can be charged with 60% efficiency (as in the case of [19]):

$$\Phi(\cdot) = \int_0^{t_f} \left[\frac{P_{se}(t) + \epsilon_{se}(t)}{2} + \frac{P_{dd}(t) + \epsilon_{dd}(t)}{2} - 0.6 \left(\frac{\epsilon_{se}(t) - P_{se}(t)}{2} + \frac{\epsilon_{dd}(t) - P_{dd}(t)}{2} \right) \right] dt \tag{11}$$

The dynamics equations, (1)-(3), were added to the path constraints of the OCP (4a), as well as the constraint to track a desired angular acceleration $\ddot{\theta}(t) + f^2 A\,\sin(f\,t) = 0$. The remaining path and boundary constraints, namely torque limits, initial and periodicity conditions, are reported in a companion technical report [20].

C. 2-DoF: MODEL

The dynamics equations of the 2-DoF manipulator [21] can be found in the technical report [20]. For the 2-DoF case, we introduced a small gearbox on the DD motor because of the demanding torque requirements. Thus, what previously was called DD, is now referred to as Quasi-Direct Drive (QDD), since the gear ratio was limited to 10 [22].

D. 2-DoF: OCP FOR CO-DESIGN

The energy consumption analysis begins by considering the swing-up problem, illustrated in Fig. 2. It consists of making the manipulator lift a weight from the downward vertical configuration ($\theta_1(0) = -\pi/2,\ \theta_2(0) = 0$) up to the upward vertical one $\big(\theta_1(t_f) = \pi/2,\ \theta_2(t_f) = 0\big)$. Thus, we formulated an OCP to minimize both the energy consumed and the time to complete this task. In an industrial context, task completion time and energy consumption both impact profits. We used weights w_1 and w_2 in the cost function to set the relative importance of these two quantities. The choice of minimizing a single objective function, rather than performing a multi-objective optimization, was taken in light of the fact that both energy and time can be converted into money, using appropriate weights. Thus, carefully selecting the weights based on the type of company considered, the solution to our co-design problem represents the choice that minimizes the overall cost that the company has to bear for the design and control of such a robotic system achieving the task considered. In this 2-DoF case, some simplifying assumptions taken in the 1-DoF case were abandoned. Indeed, the inertias of gearboxes and QDD motors, as well as the viscous friction of joints and motors, were considered in the dynamics equations of the system [20]. For the sake of completeness, we first investigated the case with no energy regeneration, and then the case with it. The co-design OCP is formulated as:

$$\underset{t_f, x(t), u(t), \rho}{\text{minimize}}\ \Phi\left(t_f, x(t_f), u(t_f), \rho\right) \tag{12a}$$

$$\text{subject to } \dot{x}(t) = f(t, x(t), u(t), \rho) \tag{12b}$$

$$h(t, x(t), u(t), \rho) \leq 0 \tag{12c}$$

$$g(t_f, x(0), x(t_f/2), x(t_f), \rho) \leq 0 \tag{12d}$$

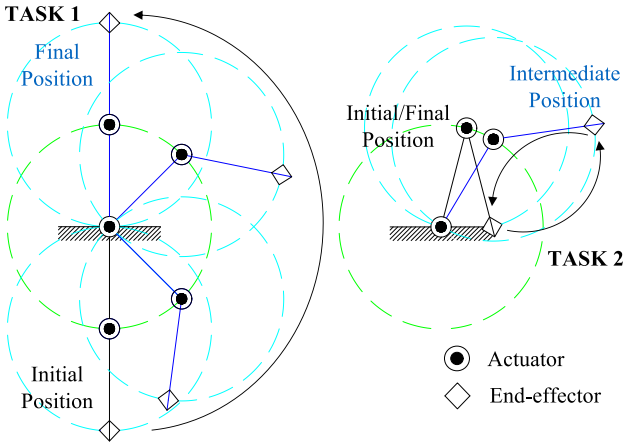

FIGURE 2. Swing-up task and pick-and-place operation performed by the 2-DoF system. The green and blue circles represent instantaneous position domains for the first and second link, respectively.

The key aspect making this problem one of co-design is the additional decision variables in ρ, which contains the design parameters: motor masses, spring stiffnesses and gear ratios. The motor constant and inertia of each motor were related to the motor mass by the relationships presented in [15] and reported in the technical report [20]. Detailed path and boundary constraints (12c) and (12d) are provided in [20] as well.

Without energy regeneration, the expression of the cost function (12a) is:

$$\Phi(\cdot) = w_1 \int_0^{t_f} \left(\sum_{k=1}^{2} \frac{P_{se,k}(t, \rho) + \epsilon_{se,k}(t, \rho)}{2} \right. \tag{13}$$

$$\left. + \sum_{k=1}^{2} \frac{P_{dd,k}(t, \rho) + \epsilon_{dd,k}(t, \rho)}{2} \right) dt + w_2 t_f^2 \tag{14}$$

To avoid trivial solutions that would have exploited only the torque given by the pre-load of the SEAs springs, for this task we set the pre-load to zero.

The effects of this redundant actuation were also studied considering a pick-and-place operation for a 2-DoF manipulator (see Fig. 2). The task consists of moving the manipulator from an initial configuration to a certain position of the end-effector, and then bringing it back to the initial configuration. Specifically, the initial/final configuration is given by the end-effector being at the same height of the first joint and at a distance of $l_1/2$ from it, while in the intermediate configuration the end-effector reaches a height of l_1 and a distance of $3l_1/2$.

For this task, we let the springs pre-load remain free, but added a constraint that the final pre-load must be equal to the initial one.

III. RESULTS

This section reports the results for the 1-DoF and 2-DoF models. First, we compare the energy consumption of the redundant actuator and SEA for the 1-DoF system. We found that for sinusoidal motions the energy saving using the redundant actuation can exceed 90%. Moreover, the resulting optimal control strategy is very similar to the latching control used in energy harvesters [17], [18], which consists in locking the moving body of a heaving buoy device at the end of the oscillation, so when its velocity is zero, and then releasing it when its velocity is back in phase with the wave excitation force.

With the 2-DoF system, the comparison extends also to GMs (*i.e.*, DC motors attached to gearboxes with gear ratios up to $N = 200$), redundant actuation at both the joints, and redundant actuation at the first joint and SEA at the second joint. The 2-DoF system carried out two different tasks: swing-up and pick-and-place. A co-design framework was built to find optimal hardware parameters and control trajectories for each task. Our analysis shows that, even though latching-like control is not optimal for nonsinusoidal motions, the redundant actuation can still be more efficient than SEAs and GMs.

In addition, we studied also the closed-loop behavior of the actuators under perturbations. We found that tracking the

desired trajectories while maintaining low energy consumption can sometimes be facilitated by the actuator redundancy.

A. 1-DoF: TEST DETAILS

The test with the 1-DoF system consists of fixing the motion of the joint (sinusoid) and optimizing the redundant actuation control to minimize the energy consumption. In the case with only the SEA, the motor torque is analytically determined. The frequency range in the analysis goes from 0.1 to 10 Hz, with 0.1 Hz resolution. The set of values for the spring stiffness is [30, 50, 100] Nm/rad, while for the gear ratio of the SEA it is [5, 10, 15, 20, 30, 50, 100, 150, 200].

The same brushless DC motor model was considered for both the SEA and the DD motor. Motor specifications include: peak torque $\tau_{max} = 7.13\,\text{Nm}$, rotor inertia $I_{se} = 10^{-5}\,\text{kg}\cdot\text{m}^2$ and motor constant $K_m = 0.64\,\text{Nm}/\sqrt{\text{Watt}}$. The gearbox efficiency was considered to scale exponentially with the gear ratio as suggested in [15].

For all the possible combinations of oscillation frequency, spring stiffness and gear ratio, the OCP (4a) was specified using the optimization modeling language PYOMO [23], [24] and solved using IPOPT [25] with the MA57 linear solver [26]. The OCP was transcribed using direct collocation with a Lagrange-Radau scheme, 30 finite elements, and 3 collocation points per element.

B. 1-DoF: TEST RESULTS

Our results show that the redundant actuation is energetically more efficient than the SEA. Fig. 3 shows the energy consumption of the SEA, considering a 30 Nm/rad spring stiffness and different gear ratios, while Fig. 4 shows the case with redundant actuation. Both cases assumed no energy regeneration. The valleys in Fig. 3 occur at the system natural frequencies, which vary depending on the gear ratio. Indeed, the higher the gear ratio, the lower the system natural frequency. The natural frequency also depends also on the spring stiffness: fixing the gear ratio, the natural frequency shifts to higher values as the spring stiffness increases.

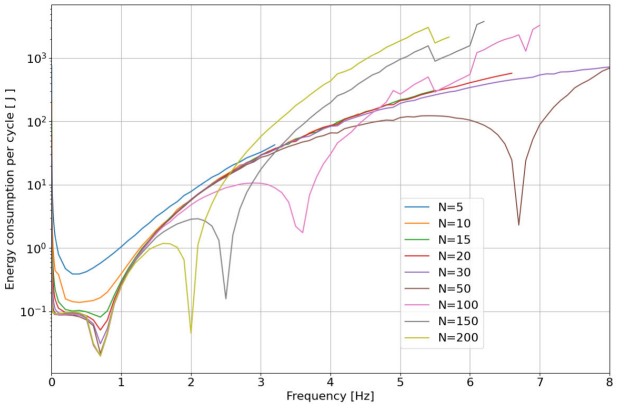

FIGURE 3. Energy use as a function of the oscillation frequency for the SEA with spring constant $K_s = 30\,\text{Nm/rad}$ and 9 different gear ratios N.

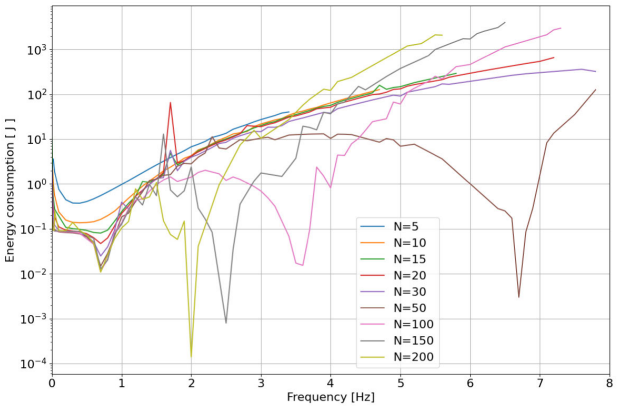

FIGURE 4. Energy use as a function of the oscillation frequency for the redundant actuator with spring constant $K_s = 30\,\text{Nm/rad}$ and 9 different gear ratios N.

To better understand the energy advantage of the redundant actuation, Fig. 5 shows the energy savings achieved with the redundant actuation in absolute terms while Fig. 6 illustrates the energy savings as a percentage of the

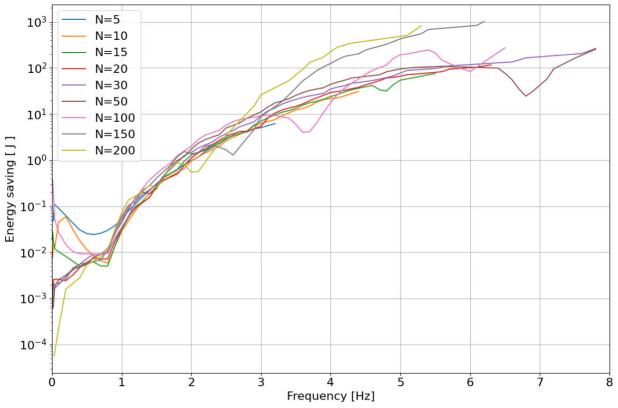

FIGURE 5. Energy saving of the redundant actuation expressed in absolute values.

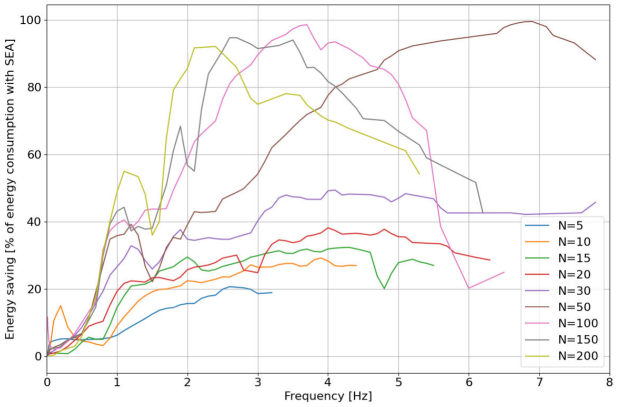

FIGURE 6. Energy saving of the redundant actuation expressed as percentage of SEA energy consumption.

SEA energy consumption. To improve readability, we filtered the data of Fig. 5 and Fig. 6 with a digital Butterworth filter of order 1 with critical frequency equal to 0.2 half-cycles/s (sampling frequency = 2 half-cycles/s). The energy savings can be very large, up to 99%, depending on the oscillation frequency, the gear ratio and the spring stiffness. For instance, in the range 3-4 Hz with $N = 100$ and $K_s = 30$ Nm/rad, the redundant actuation can save more than 90% of energy compared to the SEA, which means saving about 10 J. In the same frequency range, if one considers $N = 200$ then the relative energy saving decreases to about 70% but the absolute value of energy saving increases approximately to 100 J. On the other hand, at 1 Hz the energy saving is much lower: about 40% for high gear ratios ($N \geq 100$), and less than 20% for low gear ratios ($N \leq 20$).

Insight into the large energy savings achievable with the redundant actuation comes from how each actuator produces the desired joint torque. With only the SEA, the torque is provided only by the spring, while with the redundant actuation it comes also from the DD motor. The spring torque mainly stems from the motion of the SEA rotor being opposite to that of the joint. Since in this test the joint trajectory is fixed, the SEA rotor angle completely defines the spring torque. Thus, with only the SEA, the analytical solution for the rotor angle trajectory can be computed. To make the rotor achieve this motion, the motor must provide a sinusoidal torque (opposite to the spring torque which is seen as load torque by the SEA). For instance, Fig. 7 compares the torque, angular velocity, and power from the SEA and the load for $N = 100$, $Ks = 30$ Nm/rad and $f = 3$ Hz, which led to energy savings of more than 90%. As the figure shows, the SEA motor must be always powered, which implies a high energy consumption due to the SEA motor velocity reaching very high values (up to 1500 rad/s). In two large time intervals the SEA positive power (due to no energy regeneration) is greater than zero and reaches almost 100 W.

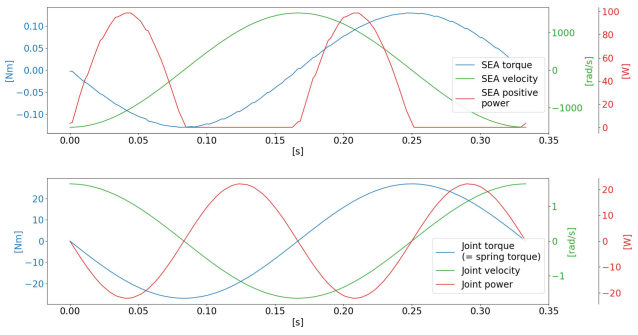

FIGURE 7. SEA: torque, velocity and power of (top) motor and (bottom) joint required to perform a 3Hz sinusoidal motion. The SEA positive power is the maximum between zero and the power consumed by the SEA (no energy regeneration case).

With the redundant actuation instead, the SEA motor is powered only during two short intervals (0.07 − 0.1 s and 0.22 − 0.26 s), when it almost halts the motion of its rotor (see Fig. 8). The SEA rotor is not completely blocked so

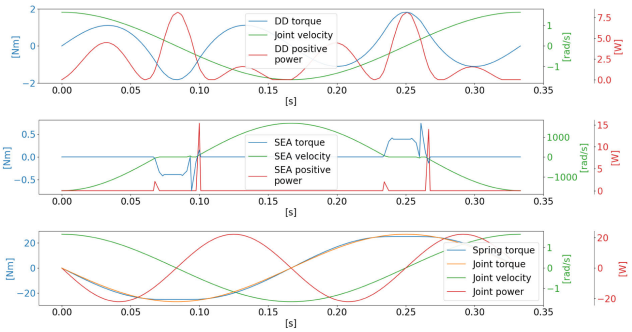

FIGURE 8. Redundant actuation: torque, velocity and power of motors and joint required to perform a 3Hz sinusoidal motion. The DD and SEA positive power is the maximum between zero and the power consumed respectively by the DD and the SEA (no energy regeneration case).

that the thermally dissipated power is compensated by negative mechanical power, resulting in nearly always nonpositive total power. It is interesting to notice that the solver found a control strategy very similar to the *latching control*, which is implemented in many energy harvesters to maximize energy generation, by keeping the SEA rotor velocity in counter-phase with the joint velocity [17], [18]. Indeed, in heaving buoy wave energy converters, the oscillating body is often latched when its velocity vanishes in order to keep the latter in phase with the wave excitation force. This condition was proved to be required for the maximization of the energy generation [27]. In the redundant actuation, this strategy is applicable thanks to the DD motor, which provides the additional torque needed to perform correctly the sinusoidal motion. Since this torque is rather small, as well as the joint velocity, the overall energy consumption remains small (peak positive power less than 8 W).

C. 2-DoF: TEST DETAILS

We considered four actuation architectures: only GMs, only SEAs, redundant actuation on both joints (Full redundant) and redundant actuation on the first joint with SEA on the second one (redundant+SEA). For both tasks, we set the weights $w_1 = 1$ (associated to energy) and $w_2 = 0.1$ (associated to time) in the cost function (14). Moreover, to improve accuracy, we increased the number of finite elements to 100. Finally, we also investigated the case with 60% energy regeneration.

Since the solution that IPOPT could find was strongly dependent on the initial guess of the hardware design parameters, we decided to randomize the initialization values and repeat the simulations 40 times. Beyond 40 random initial guesses, the change in the best solution was found to be negligible. To highlight the non-convexity of this co-design problem, which explains the dependency of the solution on the initial guesses, Fig. 9 illustrates the results of 40 simulations considering the pick-and-place task and the actuation architecture with only SEAs. In this case, 65% of simulations lead to the same minimum-cost solution.

TABLE 1. Task completion time and energy consumption with different actuation architectures.

Architecture	Task Time [s]		Energy [J]		Cost function	
	Swing Up	*Pick&Place*	*Swing Up*	*Pick&Place*	*Swing Up*	*Pick&Place*
GMs	5.71	3.38	226.68	42.57	229.94	43.72
SEAs	4.17	1.36	225.17	0.86	226.90	1.04
Full redundant	10.89	1.59	264.72	1.16	276.59	1.42
Redundant + SEA	5.25	1.37	214.01	0.80	216.77	0.99

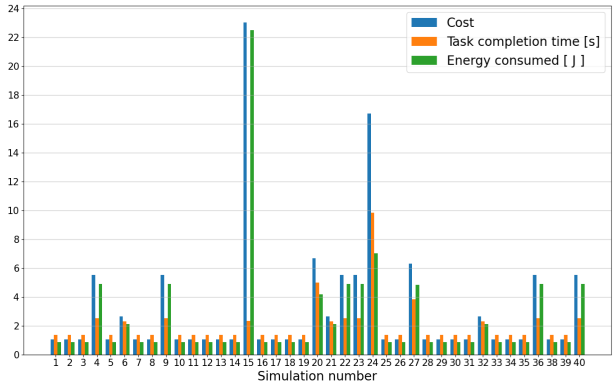

FIGURE 9. Results of 40 simulations considering the pick-and-place task and the actuation architecture with only SEAs. Because of the non-convexity of the problem, the solution strongly depends on how the decision variables are initialized.

D. 2-DoF: TEST RESULTS

1) SWING-UP

The following results concern a swing-up task with no load. Tab. 1 summarizes the results with no energy regeneration and compares the energy consumption and task completion time of the different actuation architectures. The Full redundant actuation turned out to be the least effective, in terms of both energy consumption and task completion time. Instead, the redundant+SEA configuration performed the best. It allowed for a 5% energy saving compared to only SEAs, with a 26% increase in task completion time. In contrast, when compared to only GMs, around the same energy saving comes accompanied by an 8% reduction in completion time. Tab. 1 reports also the objective function values, supporting the fact that the redundant+SEA configuration seems to be the optimal choice for the swing-up problem.

Tab. 2 lists the optimal hardware parameters found from solution of the OCP (12a) using a co-design framework. In all cases, the mass of the motors on the first joint is equal to its upper bound (10 kg), while for the motors on the second joint the optimal mass corresponds to the lower bound (0.1 kg). This is reasonable: the inertia seen at the first joint would increase if the motors on the second joint were heavier, while the motors actuating the first joint are located at the robot base and thus do not increase the inertia. The optimal gear ratios on the second joint in both cases with GMs and with Full redundant actuation are at the lower bound, namely 1. Therefore, the GM and QDD at the second joint contribute

TABLE 2. Co-design results for swing up task.

Architecture	Motor Mass [kg]		Gear Ratio		Spring Stiffness
	GM	*QDD*	*GM*	*QDD*	*[N·m/rad]*
1^{st} GM	10.00	—	18.79	—	—
2^{nd} GM	0.10	—	1.00	—	—
1^{st} SEA	10.00	—	21.25	—	139.12
2^{nd} SEA	0.10	—	200.00	—	17.21
1^{st} Redundant	10.00	10.00	8.51	8.47	43.61
2^{nd} Redundant	0.10	0.10	200.00	1.00	74.88
1^{st} Redundant	10.00	0.10	13.35	10.00	70.65
2^{nd} SEA	0.10	—	200.00	—	24.75

very little to the motion, while considerably increasing the inertia of the system; for this reason the solver sets also the motor masses to the lower bound.

This finding motivated us to investigate the design with redundant actuation at the first joint and only SEA at the second one. That the optimal gear ratios of the SEAs on the second joint are at their upper bound means that the solver tries to maximize the contribution of these SEAs without increasing the inertia of the system. However, if the gearbox mass was modelled as function of the gear ratio, then the optimal gear ratios would be lower than 200 because they would affect directly the system inertia and so the energy use.

2) PICK AND PLACE

Tab. 1 summarizes the results of the pick-and-place operation. The three actuation systems that employ SEAs clearly outperform the one with GMs. This is due to the task periodicity, which enables exploiting the springs pre-load to perform the motion. As observed with the swing-up task, also in this case the best results are achieved using the redundant actuation on the first joint and SEA on the second one. Compared to the Full redundant actuation, the energy savings is 31% and the completion time is reduced by 13.8%. Considering the case with only SEAs instead, the task can be performed taking almost the same time but consuming 7% less energy.

Tab. 3 presents the resulting optimal hardware parameters for the pick-and-place task. As observed with the swing-up task, in all cases the optimal mass of the motors on the first joint is the maximum allowed, as it happens also for the gear ratios of the SEAs on the second joint, while the optimal motor mass of the QDD on the second joint of the Full redundant actuation as well as its gear ratio hit the lower bounds. The fact that the values of gear ratio of the SEAs on the first joint are equal to their upper bound may be due to the high-torque demanding static conditions set for this task

TABLE 3. Co-design results for pick&place task.

Architecture	Motor Mass [kg]		Gear Ratio		Spring Stiffness
	GM	*QDD*	*GM*	*QDD*	*[N·m/rad]*
1^{st} GM	10.00	—	89.41	—	—
2^{nd} GM	4.34	—	10.71	—	—
1^{st} SEA	10.00	—	200.00	—	250.00
2^{nd} SEA	3.17	—	200.00	—	9.23
1^{st} Redundant	10.00	10.00	200.00	5.66	250.00
2^{nd} Redundant	2.75	0.10	200.0	1.00	5.51
1^{st} Redundant	10.00	10.00	200.00	4.52	250.00
2^{nd} SEA	3.18	—	200.00	—	9.18

in the initial-intermediate-final configurations. With this task, it is not convenient to adopt the strategy of using the SEAs to store and release mechanical power through the swinging motion of the links, as in the case of the swing-up task. This may explain why the solver sets the spring stiffnesses of the SEAs on the first joint to the maximum value, so as to increase the bandwidth of the SEAs.

As presented so far, the co-design results for both tasks show that the hardware design parameters hit the upper or lower bounds many times. Whereas in some cases this phenomenon can be explained quite easily, in other cases finding an intuitive explanation is much more complicated and the results may actually be misleading. A solution to this problem could be the use of regularization terms in the cost function that prevent those hardware parameters from hitting their upper and lower bounds.

The results up to this point suggest that a periodic task can be efficiently achieved in ideal settings using SEAs, thanks to their capability to store and release mechanical power without wasting energy. The benefits of adding a DD in parallel to the SEA in the 1-DoF system, that allows for a latching control strategy, were observed only to a small extent with the 2-Dof system and the tasks considered. Nonetheless, choosing other tasks may highlight more effectively the energy efficiency of the redundant actuation.

E. 2-DoF: FEEDBACK CONTROL

The previous subsections investigated the energy efficiency of different actuation architectures (SEA, GM, Full redundant, redundant+SEA) in ideal settings, showing that the redundant actuator and redundant+SEA can lead to energy savings. However, this does not suffice to claim that this actuator could perform well in the real world. For this reason, we now analyse how different actuators behave in more realistic settings, in which the system has to cope with modeling errors and disturbances using feedback control.

To this end, we used a PD controller with hand-tuned gains to observe how energy consumption and task completion accuracy varied due to modeling errors in the hardware parameters and joint acceleration disturbances. We carried out 10 simulations for each actuation system, randomly selecting the magnitude of the disturbances up to 1% of the nominal value of the optimized hardware parameters and considering impulsive variations of the joint accelerations ($10\,\mathrm{rad/s^2}$) randomly occurring between 25% and 75% of the task completion time. Figs. 10 and 11 show the energy consumption and the maximum joint state error for the pick-and-place operation and swing-up task, respectively. The error is measured at the intermediate and final state for the pick-and-place task and only at the final state for the swing-up task. The dashed vertical lines represent the energy consumption in absence of any disturbance, while the dashed horizontal line is a subjective threshold representing the maximum position error (0.5°) below which we consider the task successful. Since nominal energy consumption with only SEAs and with redundant+SEA are very similar (respectively 0.86 J and 0.80 J), the corresponding lines overlap.

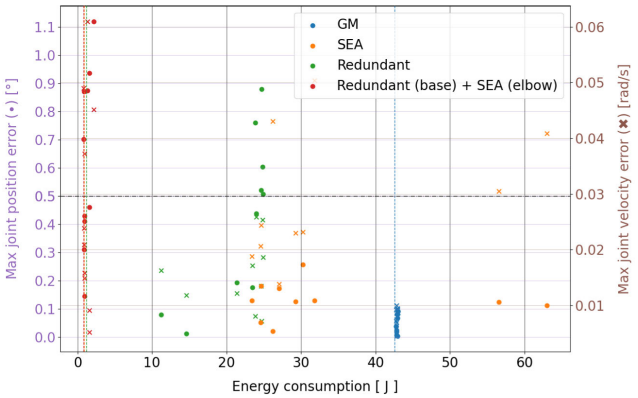

FIGURE 10. Pick-and-Place Task: energy consumption and maximum between intermediate and final joint-state error with PD control and disturbances in the optimized hardware parameters as well as impulsive variations of joint accelerations The dots and crosses mark the position and velocity error against energy, respectively.

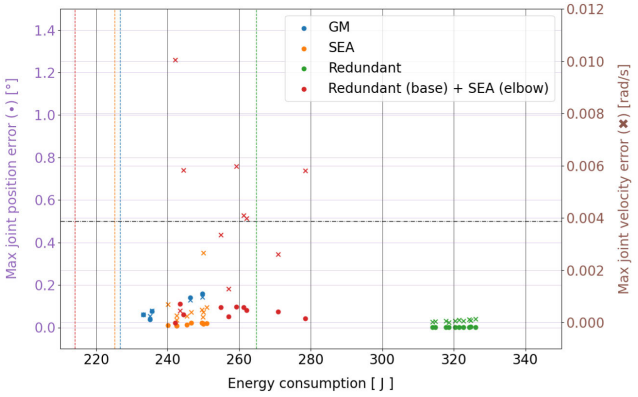

FIGURE 11. Swing-Up Task: energy consumption and maximum final joint-state error with PD control and disturbances in the optimized hardware parameters as well as impulsive variations of joint accelerations. The dots and crosses mark the position and velocity error against energy, respectively.

In the pick-and-place task, the open-loop behavior of the system with redundant+SEA also extends to closed-loop with disturbances: the energy consumption is very close to the nominal one, although the maximum joint position error exceeds the threshold in half of the simulations. The GM actuation also ensures an energy consumption very close to

the nominal one, in addition to an overall high accuracy and precision. The other two actuation systems instead perform poorly both in terms of actual energy consumption and task accuracy. Overall, the maximum position and velocity errors considering the intermediate and final configurations remain consistently bounded.

The results are different for the swing-up task: SEA and redundant+SEA perform similarly, while good accuracy is obtained with Full redundant actuation to the detriment of a high increment in energy consumption. In Fig. 11, the results of only 5 simulations with GMs are shown because in half of the simulations the controller failed to stabilize the system. In terms of accuracy compared to the pick-and-place task, the results for the swing-up task may be explained by the instability of the desired final configuration. An exception is represented by the Full redundant actuation, which may benefit from the combined action of QDD and SEA on the second joint to better reject acceleration disturbances.

IV. CONCLUSION

This study presented an energy efficiency analysis of a redundant actuation system based on a co-design framework. The analysis started from a simple case study, which examines the energy consumption of an oscillating 1-DoF system. A frequency study was carried out to investigate the behavior of the redundant actuation compared to a SEA in terms of energy consumption. Then we focused on a 2-DoF planar manipulator. We considered two tasks and used co-design to make optimal choices in the simultaneous design of hardware and control. Finally, we investigated the closed-loop behavior of the different actuation systems subject to modeling errors and disturbances using PD control to track the previously computed optimal trajectories.

The results show that the proposed redundant actuation is energetically convenient compared to standard actuators as GMs or SEAs. With the 1-DoF system performing a sinusoidal motion, the energy savings compared to an SEA can be very large, sometimes exceeding 90%. For the 2-DoF system instead, the energy savings turns out to be task dependent, but in any case the optimal configuration seems to consist of having redundant actuation on the first joint and an SEA on the second one. This system can outperform GMs (up to 99% energy consumption reduction), but it leads to limited savings (up to 7%) with respect to only SEAs. This finding suggests that transmission designs (e.g., as in [28]) relating sinusoidal angle/torque input trajectory of the actuator to nonsinusoidal output trajectories might be pursued to enable significant energy savings for other behaviors. In addition, for a pick-and-place task, the energetic advantages of the redundant actuation also extend to closed-loop control with perturbations. With the proposed co-design framework, it was possible not only to study and verify the energy convenience of this redundant actuation, but also to obtain optimal values for its hardware parameters and optimal state-control trajectories. Furthermore, co-design shows that there is increased incentive for adopting redundant actuation for more proximally located joints. This suggests that the importance of designing transmission systems to relay power distally will be even more important for designs adopting redundant actuation schemes.

To improve the analysis of closed-loop energy efficiency for different actuation systems, future work will explore the possibility of computing optimal feedback gains using parametric optimization as well as the use of more advanced control methods such as Model Predictive Control. Another future development will be the extension of this study to a single leg of a quadruped subject to different gaits, obtaining optimal hardware designs and control trajectories via simulation, and analyzing the energy efficiency of diverse actuation configurations in a real application. Finally, a mixed-integer OCP could be formulated to let the solver choose which actuation system is the best to actuate each single joint.

REFERENCES

[1] G. A. Pratt and M. M. Williamson, "Series elastic actuators," in *Proc. IEEE/RSJ Int. Conf. Intell. Robots Syst.*, Pittsburgh, PA, USA, Aug. 1995, pp. 399–406.
[2] C. Lee, S. Kwak, J. Kwak, and S. Oh, "Generalization of series elastic actuator configurations and dynamic behavior comparison," *Actuators*, vol. 6, pp. 1–26, Aug. 2017.
[3] S. Seok, A. Wang, D. Otten, and S. Kim, "Actuator design for high force proprioceptive control in fast legged locomotion," in *Proc. IEEE/RSJ Int. Conf. Intell. Robots Syst.*, Vilamoura, Portugal, Oct. 2012, pp. 1970–1975.
[4] P. M. Wensing, A. Wang, S. Seok, D. Otten, J. Lang, and S. Kim, "Proprioceptive actuator design in the MIT cheetah: Impact mitigation and high-bandwidth physical interaction for dynamic legged robots," *IEEE Trans. Robot.*, vol. 33, no. 3, pp. 509–522, Jun. 2017.
[5] G. Kenneally, A. De, and D. E. Koditschek, "Design principles for a family of direct-drive legged robots," *IEEE Robot. Autom. Lett.*, vol. 1, no. 2, pp. 900–907, Jul. 2016.
[6] A. G. Leal, R. M. D. Andrade, and A. B. Filho, "Series elastic actuator: Design analysis and comparison," *Recent Adv. Robot. Syst.*, vol. 1, pp. 203–234, Sep. 2016.
[7] K. Y. H. Toumi Asada, *Direct-Drive Robots, Theory and Practice*. Cambridge, MA, USA: MIT Press, 1987.
[8] M. Zinn, B. Roth, O. Khatib, and J. K. Salisbury, "A new actuation approach for human friendly robot design," *Int. J. Robot. Res.*, vol. 23, nos. 4–5, pp. 379–398, Apr. 2004.
[9] J. B. Morrell and J. K. Salisbury, "Parallel-coupled micro-macro actuators," *Int. J. Robot. Res.*, vol. 17, no. 7, pp. 773–791, Jul. 1998.
[10] K. Sims, "Evolving virtual creatures," in *Proc. 21st Annu. Conf. Comput. Graph. Interact. Techn. (SIGGRAPH)*, Orlando, FL, USA, 1994, pp. 15–22.
[11] N. Cheney, R. MacCurdy, J. Clune, and H. Lipson, "Unshackling evolution: Evolving soft robots with multiple materials and a powerful generative encoding," in *Proc. 15th Annu. Conf. Genet. Evol. Comput. Conf. (GECCO)*, Amsterdam, The Netherlands, 2013, p. 167.
[12] K. M. Digumarti, C. Gehring, S. Coros, J. Hwangbo, and R. Siegwart, "Concurrent optimization of mechanical design and locomotion control of a legged robot," in *Proc. 17th Int. Conf. Climbing Walking Robots (CLAWAR)*, Poznan, Poland, Jul. 2014, pp. 315–323.
[13] J. Hass, J. M. Herrmann, and T. Geisel, "Optimal mass distribution for passivity-based bipedal robots," *Int. J. Robot. Res.*, vol. 25, no. 11, pp. 1087–1098, Nov. 2006.
[14] Q. Li, W. J. Zhang, and L. Chen, "Design for control—A concurrent engineering approach for mechatronic systems design," *IEEE/ASME Trans. Mechatronics*, vol. 6, no. 2, pp. 161–169, Jun. 2001.
[15] Y. Yesilevskiy, Z. Gan, and C. D. Remy, "Energy-optimal hopping in parallel and series elastic one-dimensional monopeds," *J. Mech. Robot.*, vol. 10, no. 3, pp. 4–5, Jun. 2018.
[16] G. Bravo-Palacios, A. D. Prete, and P. M. Wensing, "One robot for many tasks: Versatile co-design through stochastic programming," *IEEE Robot. Autom. Lett.*, vol. 5, no. 2, pp. 1680–1687, Apr. 2020.

[17] A. Babarit and A. H. Clément, "Optimal latching control of a wave energy device in regular and irregular waves," *Appl. Ocean Res.*, vol. 28, no. 2, pp. 77–91, Apr. 2006.
[18] F. Saupe, J. C. Gilloteaux, P. Bozonnet, Y. Creff, and P. Tona, "Latching control strategies for a heaving buoy wave energy generator in a random sea," in *Proc. 19th IFAC*, Cape Town, South Africa, Aug. 2014, pp. 7710–7716.
[19] A. Adib and R. Dhaouadi, "Modeling and analysis of a regenerative braking system with a battery-supercapacitor energy storage," in *Proc. 7th Int. Conf. Modeling, Simulation, Appl. Optim. (ICMSAO)*, Cape Town, South Africa, Apr. 2017, pp. 1–6.
[20] G. Grandesso, G. Bravo-Palacios, P. M. Wensing, M. Fontana, and A. D. Prete, "Exploring the limits of a hybrid actuation system through co-design," Dept. Ind. Eng., Univ. Trento, Trento, Italy, Tech. Rep., 2020. [Online]. Available: https://hal.archives-ouvertes.fr/hal-02737086
[21] M. W. Spong, "The swing up control problem for the Acrobot," *IEEE Control Syst.*, vol. 15, no. 1, pp. 49–55, Feb. 1995.
[22] N. Kau, A. Schultz, N. Ferrante, and P. Slade, "Stanford doggo: An open-source, quasi-direct-drive quadruped," in *Proc. Int. Conf. Robot. Autom. (ICRA)*, Montreal, QC, Canada, May 2019, pp. 6309–6315.
[23] W. E. Hart, J.-P. Watson, and D. L. Woodruff, "Pyomo: Modeling and solving mathematical programs in Python," *Math. Program. Comput.*, vol. 3, no. 3, pp. 219–260, Aug. 2011.
[24] W. E. Hart, C. Laird, J. Watson, D. L. Woodruff, G. A. Hackebeil, B. L. Nicholson, and J. D. Siirola, *Pyomo—Optimization Modeling in Python*, 2nd ed. Cham, Switzerland: Springer, 2017.
[25] A. Wächter and L. T. Biegler, "On the implementation of an interior-point filter line-search algorithm for large-scale nonlinear programming," *Math. Program.*, vol. 106, no. 1, pp. 25–57, Mar. 2006.
[26] (2013). *HSL: A Collection of Fortran Codes for Large Scale Scientific Computation*. [Online]. Available: http://www.hsl.rl.ac.uk
[27] K. Budal and J. Falnes, "Interacting point absorbers with controlled motion," in *Power From Sea Waves*, B. M. Count, Ed. London, U.K.: Academic, 1980, pp. 381–399.
[28] S. Coros, B. Thomaszewski, G. Noris, S. Sueda, M. Forberg, R. W. Sumner, W. Matusik, and B. Bickel, "Computational design of mechanical characters," *ACM Trans. Graph.*, vol. 32, no. 4, pp. 1–12, Jul. 2013.

GIANLUIGI GRANDESSO received the B.S. degree in industrial engineering and the M.S. degree (Hons.) in mechatronics engineering from the University of Trento, Trento, Italy, in 2016 and 2019, respectively, where he is currently pursuing the Ph.D. degree with the Department of Industrial Engineering.

He is also undertaking research on the concurrent design of hardware and control of high-performance robotic systems, with a focus on combining deep reinforcement learning methods with trajectory optimization. His principal research interests include robot design, optimal control, and reinforcement learning. He received the MIUR Departments of Excellence Scholarship for his Ph.D. Degree.

GABRIEL BRAVO-PALACIOS (Graduate Student Member, IEEE) received the B.S. degree in mechanical engineering from the Escuela Politécnica Nacional, Quito, Ecuador, in 2012, and the M.S. degree in mechanical engineering from Iowa State University, Ames, IA, USA, in 2015. He is currently pursuing the Ph.D. degree with the Robotics, Optimization and Assistive Mobility (ROAM) Laboratory, Department of Aerospace and Mechanical Engineering, University of Notre Dame, Notre Dame, IN, USA.

He is also a member of the Robotics, Optimization and Assistive Mobility (ROAM) Laboratory, Department of Aerospace and Mechanical Engineering, University of Notre Dame. His current research interest includes the computational design of legged robots and robotic manipulators, emphasizing the concurrent optimization of hardware and control systems.

PATRICK M. WENSING (Member, IEEE) received the B.S., M.S., and Ph.D. degrees in electrical and computer engineering from The Ohio State University, Columbus, OH, USA, in 2009, 2013, and 2014, respectively.

He is currently an Assistant Professor with the Department of Aerospace and Mechanical Engineering, University of Notre Dame, where he directs the Robotics, Optimization, and Assistive Mobility (ROAM) Laboratory. Before joining Notre Dame, he was a Postdoctoral Associate with MIT, working on control system design for the MIT cheetah robots. His current research interest includes aspects of dynamics, optimization, and control toward advancing the mobility of legged robots and assistive devices. He received the NSF CAREER Award (2020) and has been recognized with multiple best paper awards for his work. He also serves as the Co-Chair for the IEEE RAS Technical Committee on Model-Based Optimization for Robotics and an Associate Editor for the IEEE TRANSACTIONS ON ROBOTICS.

MARCO FONTANA (Member, IEEE) received the M.S. degree in 2003 and the Ph.D. degree in 2008.

He is currently an Associate Professor of mechanical engineering with Scuola Superiore Sant'Anna, Pisa, Italy, where he leads the Robotic Mechanisms and Materials Group. He has been a coordinator of different national and international research initiatives and projects. He is the author of more than 70 papers appeared in international conference proceedings and ISI journal in the field of mechatronics and smart materials and five book chapters. He is the inventor of five international patents. His research interests include innovative basic concepts and solutions for mechatronic systems, robotics, and energy harvesting devices.

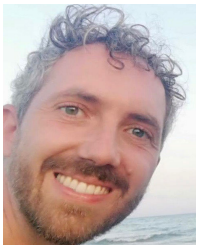

ANDREA DEL PRETE (Member, IEEE) received the degree (Hons.) in computer engineering from the University of Bologna, Bologna, Italy, in 2009, and the Ph.D. degree in robotics from the Cognitive Humanoids Laboratory, Italian Institute of Technology, Genova, Italy, in March 2013.

From 2014 to 2017, he was a Postdoctoral Researcher with Laboratoire d'Analyse et d'Architecture des Systemes, CNRS, Universite de Toulouse, Toulouse, France, working on optimization-based control of the humanoid robot HRP-2. In 2018, he had worked as a Senior Researcher with the Max Planck Institute for Intelligent Systems, Tübingen, Germany. Since 2019, he has been an Assistant Professor with the University of Trento, Trento, Italy.